H13-219

CORRIDORS OF ENHANCED TRANSPORT AND DISPERSION: GLOBAL DISTRIBUTION AND CHARACTERISTICS

Daran Rife[1], James Pinto[1], Andrew Monaghan[1], Christopher Davis[1], and John Hannan[2]

[1]National Center for Atmospheric Research, Boulder, Colorado, USA
[2]Defense Threat Reduction Agency, Ft. Belvoir, VA, USA

Abstract: This paper documents the global distribution and characteristics of corridors of enhanced transport and dispersion (T&D), particularly their diurnal and vertical structure. These corridors, generically termed low-level jets (LLJs), are ubiquitous features within the world's land covered areas, and regularly occur during the warm season. To accomplish this goal, a new 21-year global reanalysis was performed with an MM5-based global climate downscaling system using a grid spacing of 40 km. A unique characteristic of the reanalysis is the availability of hourly three-dimensional output, which permits the full diurnal cycle to be analyzed. The first available objectively constructed global maps of recurring NLLJs are created, where the various NLLJs can be simultaneously viewed at or near their peak time. These maps not only highlight all the locations where NLLJs are known to recur, but also reveal a number of new jets.
The authors examine the basic mechanisms that give rise to the NLLJs identified in two disparate locations, each having a profound influence on the regional T&D, and illustrate the variety of physiographic and thermal forcing mechanisms that can produce NLLJs. The shallowness of the jets, their dependence on turbulence, their ubiquity and intensity underscore a fundamental challenge to global weather and T&D modeling of the distribution of atmospheric constituents originating from the Earth's surface and human activity.

Key words: *Low-level jets, Transport and dispersion, Planetary boundary layer, Climate downscaling, MM5.*

INTRODUCTION

Worldwide, a central influence on human activity is the transport of water vapor and other atmospheric constituents from low to high latitudes, or directly from warm oceans inland over continents. Much of this transport occurs within confined wind corridors termed generically as low-level jets (LLJs). As outlined in the review by Stensrud (1996, hereafter S96) these jets take many forms. Perhaps the most commonly studied LLJs are those that maximize at night. The so-called nocturnal LLJ (NLLJ) is a nearly ubiquitous feature, some of which have a dramatic effect on transport near metropolitan areas. Studies by Mao and Talbot (2004) and Darby *et al.* (2006) show how a nocturnal jet occurring a few hundred meters above the ground can transport urban-generated chemicals well outside the urban area. NLLJs such as the low-level jet of the Great Plains of North America have been the subject of intensive study (e.g., S96), as has the South American NLLJ (Vera *et al.* 2006; Salio *et al.* 2007). S96 also noted jets in other locations around the world, including Australia, South Africa, the Indian subcontinent, and southeast Asia. However, these jets have been studied much less.

The study focuses on jets that have an along-jet scale of several hundred kilometers, and therefore exert a profound influence upon the regional weather and T&D. Our goal is to emphasize the underlying commonalities of the jets, using a 21-year global reanalysis performed with the MM5 model using a horizontal grid spacing of 40 km. Low-level jets with substantial diurnal variability have traditionally been difficult to study from a global perspective because of the lack of spatial and temporal resolution of available global reanalyses. A unique characteristic of the reanalysis used in this study is the availability of hourly output. This allows the full diurnal cycle to be analyzed. Furthermore, with a horizontal grid spacing of 40 km, many topographic features are better resolved than in widely used global datasets such as the NCEP-NCAR Reanalysis (NNRP). Thus, the diurnal variation of NLLJs, as well as the local forcing, is well represented in our analysis. This makes possible a detailed examination of the systematic onset and cessation of the jets, including time-height representations of the diurnal cycle.

Global maps of NLLJ activity are developed, based on the temporal variations in the wind's vertical profile, defined in local time. This allows us to simultaneously view the objectively defined NLLJs index and thus have a quantitative analogue of Fig. 1 given in S96. This index is defined and applied to document the global occurrences of NLLJs. A representative case for one NLLJ is presented to better understand the mechanisms that produce these jets.

GLOBAL DYNAMICALLY DOWNSCALED ANALYSIS

A global mesoscale reanalysis with hourly temporal resolution in three dimensions was created for this study, which permits the diurnal cycle to be fully resolved. This analysis utilizes NCAR's Climate Four Dimensional Data Assimilation system (CFDDA; Hahmann *et al.* 2010). CFDDA is a dynamical downscaling system developed by NCAR to generate high-resolution climatographic analyses for any part of the world. At the heart of CFDDA is NCAR's Real Time Four Dimensional Data Assimilation system (RTFDDA; Liu *et al.* 2008), a mesocale-model-based assimilation and forecasting system with versions based upon both the MM5 and its sequel, the Weather Research and Forecast (WRF) Model. For the application described herein, we use the MM5-based version of CFDDA (MM5 version 3.6) to create global hourly analyses on a 40-km horizontal grid, with 28 vertical levels covering the period 1985-2005. Full details of CFDDA's global configuration appear in Rife *et al.* (2010; R10 hereafter).

Data assimilation is accomplished using the Newtonian relaxation technique, wherein non-physical nudging terms are added to the model predictive equations (Stauffer *et al.* 1991; Stauffer and Seaman 1994). These terms force the model solution at each grid point to standard surface and upper air observations, in proportion to the difference between the model solution and the data. This approach is used because it is computationally efficient, it is robust, it allows the model to ingest data continuously rather than intermittently, the full model dynamics are part of the assimilation system so that analyses contain all locally forced mesoscale features. The CFDDA solution is also nudged toward the driving NCEP-DOE AMIP-II

reanalysis (NR2; Kanamitsu *et al*. 2002) at the upper levels to preserve the large-scale state in CFDDA, and to ensure mass conservation. A time invariant vertical grid nudging zone is used, from the model top down to about 3.0 km AGL (above the average height of the PBL). The underlying principle is for the CFDDA large-scale solution to closely follow that of the NR2, while not impeding the ability of the assimilated observations and CFDDA to produce small-scale features, especially within the PBL.

GLOBAL MAPS OF NLLJ ACTIVITY

Although S96 prepared a hand drawn map of LLJ locations, we seek a quantitative cartographic technique for plotting LLJs that can be applied to any gridded dataset with sufficient temporal and spatial resolution. An index of NLLJ activity is developed based upon the vertical structure of the wind's temporal variation, defined in local time. This allows us to produce the first objective maps of recurring NLLJs around the world, where the jets can be simultaneously viewed at or near their peak time. The winds at each grid point are classified as being associated with an NLLJ according to two criteria that must be satisfied simultaneously. The first requires the winds at 500 m AGL (near jet level) to be stronger at *local* midnight than at *local* noon. The second requires the wind speed at the jet's core (500 m AGL) to be stronger than that aloft (4 km AGL), similar to the criterion of Whiteman *et al.* (1997). The NLLJ index (m s^{-1}) is defined at each grid point according to

$$NLLJ = \lambda\varphi\sqrt{\left[\left(u_{00}^{L1} - u_{00}^{L2}\right) - \left(u_{12}^{L1} - u_{12}^{L2}\right)\right]^2 + \left[\left(v_{00}^{L1} - v_{00}^{L2}\right) - \left(v_{12}^{L1} - v_{12}^{L2}\right)\right]^2}$$

where *u* and *v* are the zonal and meridional wind components, respectively. The superscripts L1 and L2 denote winds at 500 m AGL and 4000 m AGL, respectively, and represent winds within the jet core and those above the core. R10 show that the various jets are at their maximum at about 500 m AGL, consistent with the 300-600-m mean height range for the Great Plains NLLJ reported by Whiteman *et al.* (1997) and others. The subscripts 00 and 12 denote *local* midnight and *local* noon. Because the term under the square root is positive, two additional terms are needed to account for the algebraic signs of the vertical and temporal changes in the wind. The first, lambda (λ) is a binary multiplier that requires the difference between the 500 m AGL wind speed at local midnight and local noon to be positive. The second, phi (ϕ) is also a binary multiplier that requires the 500 m AGL wind speed at local midnight to be greater than that at 4000 m AGL at the same time. This ensures that the winds conform to a jet-like profile. The equations for λ and ϕ are given in R10. The result is a database of daily NLLJ index values for the entire 21-yr period, which is used to form composite global maps of NLLJ activity that highlight not only the locations for recurring jets, but also their mean strength, horizontal extent, and geographic orientation.

Figure 1 shows the 21-yr mean daily NLLJ index maps January and July. The mean 500-m-AGL wind vectors at 0000 LT are also shown (the approximate height and time of the jet maxima), to highlight the horizontal structure of the jets. The inset shows the locations of the NLLJs analyzed herein. The jets were chosen based on their known or suspected link to heavy nocturnal precipitation (Monaghan *et al.* 2010), with a special emphasis on the newly identified jets. All the known NLLJs in S96's Fig. 1 appear clearly in our objective maps, including the Great Plains NLLJ (#1), the South American NLLJ (#13 and #14), the jets over Maracaibo (#3) and N Venezuela (#2), which are part of the larger-scale Caribbean LLJ, the jet over southeast China (#10), the southerly flowing NLLJ over Baja California (not numbered), and the coast following western Australia NLLJ (#18). Most of the NLLJ maxima are evident over land areas during summer, with notable exceptions. For example, a strong NLLJ forms in Ethiopia (#17) during boreal winter, even though the jet core forms near 10° N. There are also weak NLLJs over the Brazilian Highlands in South American and east Africa's Great Rift Valley (not numbered) during austral winter, neither of which has been previously documented.

These maps show several newly identified areas of intense NLLJ activity, all lying in the northern hemisphere, and numbered in the inset of Fig. 1. These include Syria (#4), Iran (#5), Tarim Pendi (#7), Tibet (#6), Ethiopia (#17), Venezuela (#11), Guyana (#12), and Maracaibo (#3). Many of these NLLJs are associated with large moisture fluxes, while others are associated with the lofting and transport of dust. Frequency distributions of NLLJ wind speeds at each location (not shown) are strikingly similar, with most of the NLLJs having wind speeds at or below 16 m s^{-1}, and wind speeds >= 20 m s^{-1} rarely occur. The notable exception to this is the India NLLJ, whose wind speeds exceed 20 m s^{-1} about 40% of the time. The orientation of NLLJs includes all four primary directions (north, south, east and west), with the mean direction in each region depending strongly on the geographic orientation of the adjacent physiography, and the underlying horizontal heat contrasts.

Figure 2 shows the distributions of NLLJ indices at each of the locations identified in Fig. 1 for 1985-2005, to assess the jets' typical diurnal variations. Average NLLJ index values are computed within a visually defined box centered on the NLLJ's climatographical mean core for each region for the season having the strongest NLLJ (January or July) in a given location. Box sizes typically encompass a latitudinal extent of 10-15°, and a 15° longitudinal extent. The frequency distributions of most jets are remarkably similar with peaks around 10 m s^{-1}. Two jets have a particularly strong change: Iran and Tibet. The LLJ over Iran undergoes a nearly 17 m s^{-1} variation (#5; gray curve in Fig. 6a), while the Tibet LLJ typically experiences a 14 m s^{-1} daily change (#6; dashed yellow curve in Fig. 6a). The frequency distributions for the Great Plains and Argentina jets have relatively long tails. This may reflect the influence of synoptic-scale variations. The Maracaibo LLJ exhibits a much weaker frequency maximum at 5 m s^{-1} (#3; blue curve in Fig. 6a), and rarely exceeds a diurnal change of about 12 m s^{-1}.

DETAILED STUDY OF ONE NEWLY IDENTIFIED NLLJ

We focus on one of the newly identified NLLJs found over western Ethiopia (#17 in Fig. 1b). This jet occurs in Northern Hemisphere winter, although the latitude is around 10° N. The major topographic feature of the region is the Ethiopian Highlands, which extend to about 3000 m MSL (Fig. 3a). The composite analysis during the time of maximum nocturnal jet strength indicates that the north-northeasterly jet forms as easterly flow traverses the northern slopes of the Highlands (Fig.

3b) and a vortex forms in the lee. This jet rapidly accelerates around 2100 local time (Fig. 3d) and lasts through the night (Fig. 3d, Fig. 4c). The Ethiopian jet rapidly decelerates after sunrise.

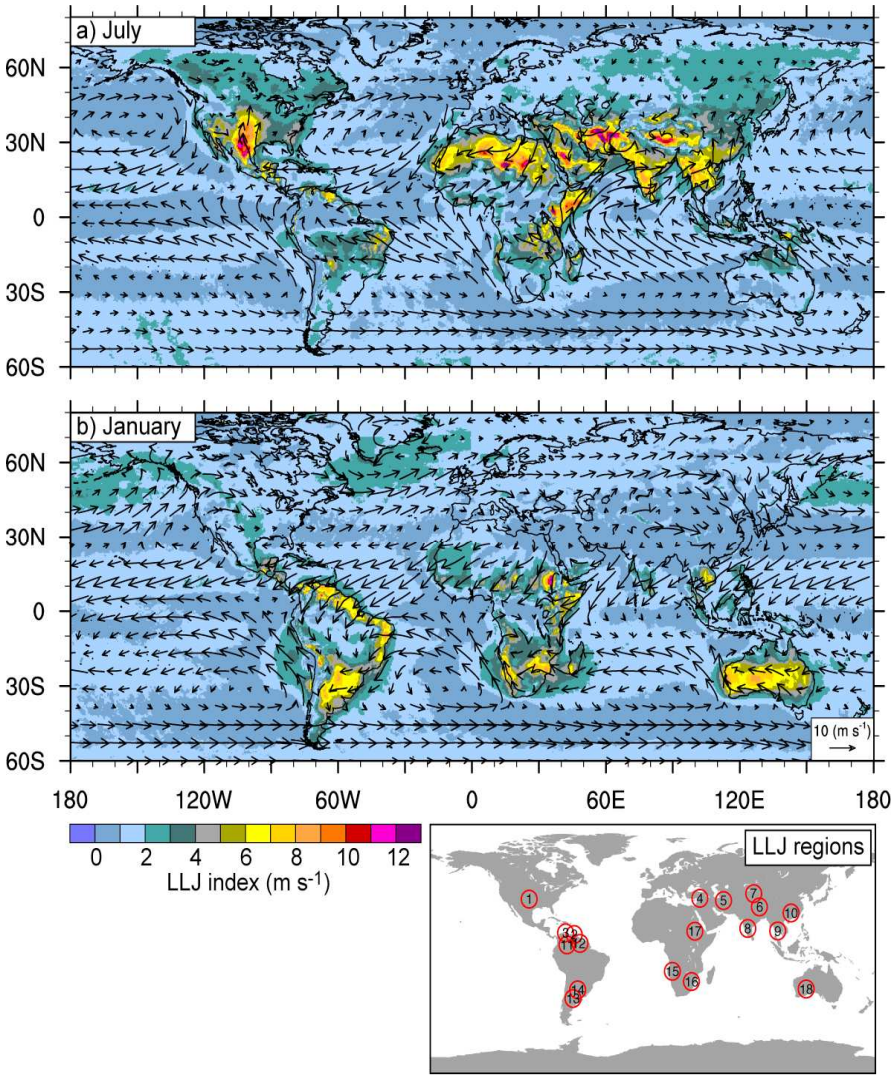

Figure 1. Mean NLLJ index (shaded) and 500 m AGL winds (arrows) at local midnight for 1985-2005 for (a) July and (b) January calculated from the CFDDA hourly analyses. The inset shows the locations of NLLJs analyzed for this study, whose characteristics are summarized in Table 2. Vector winds are plotted at approximately every twentieth grid point.

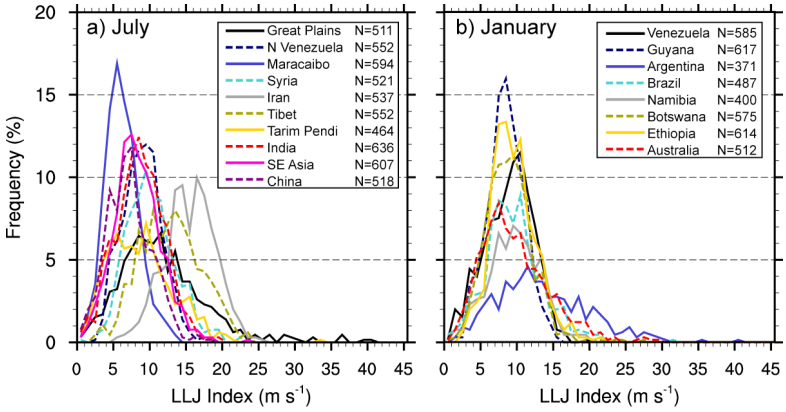

Figure 2. Distributions of NLLJ indices for the eighteen locations identified in Fig. 1 for 1985-2005 for (a) July and (b) January. The number of non-zero NLLJ index values for each region is shown in the legend. There are a total possible of 651 days (31 days × 21 years) for either July or January.

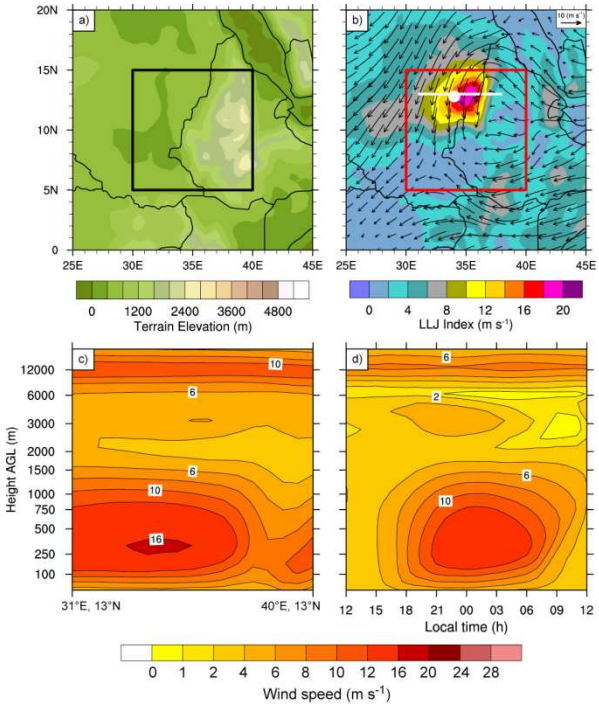

Figure 3. Composite characteristics for strong (>= 90th percentile) NLLJ events for the Ethiopia region (#17 in Fig. 1b) for July 1985-2005. (a) Terrain elevation within the region (m AMSL). (b) Mean NLLJ index (shaded) and 500 m AGL winds (arrows). Vector winds are shown at local midnight at each point, and are plotted at approximately every third grid point. Thick white line denotes the location of the cross-section shown in panel (c), and the white circle denotes the point at or near the jet core, and marks the location of the time-height plot shown in panel (d). (c) Cross-section of the mean wind speed along the white line in (b). (d) Mean time-height of wind speed within the jet core, denoted by the white circle in (b). Thick black and red lines in (a) and (b) show the visually defined box centered on the 21-year average NLLJ core.

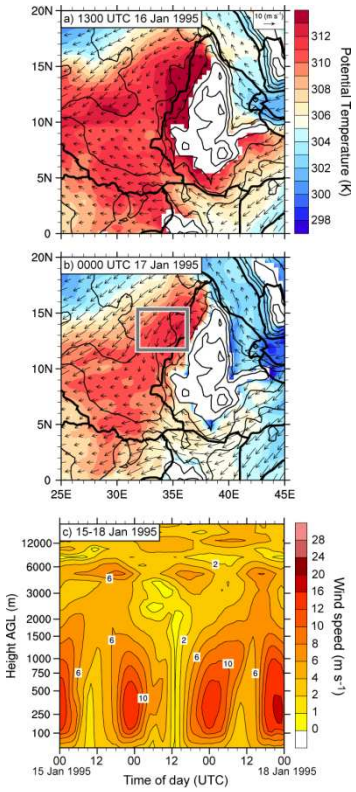

Figure 4. Characteristics of the Ethiopia NLLJ for a multi-day episode during 15-18 January 1995. (a) Potential temperature (shaded) and winds (arrows) at 850 hPa for 1300 UTC 16 Jan 1995. Thin black lines show terrain elevation in increments of 500 m. Vector winds are plotted at approximately every third grid point. (b) same as (a) but for 0000 UTC 17 Jan 1995. (c) Time-height of mean wind speed within the jet core, whose position is denoted by the white circle in Fig. 3b. Thick gray lines in (b) show the visually defined box that bounds the region of the nocturnal acceleration, and is used to calculate the horizontal momentum budget presented in Fig. 5.

We quantify the development of the nocturnal jet using a momentum budget, similar to that used by Doyle and Warner (1993). In the present case, we do not have access to the full dissipation terms, therefore, the tendencies of momentum are compared to forcing by the pressure gradient (PGF), Coriolis and advection terms. The budget represents an average over a rectangular box that bounds the region of the nocturnal acceleration. Note that even though we neglect the additional dissipation terms, their contribution is probably secondary when integrated over the development time of the jets. There is typically a slight excess of momentum forcing, which is about 5-6%. At each point within the box, the terms in the vector momentum equation are projected onto the time average of the vector wind acceleration during the roughly 12-h period that defines the spin-up of the jet. Positive values of forcing terms indicate a tendency to strengthen the jet, negative values indicate a tendency to weaken the jet.

The momentum budget for the Ethiopian jet at 900 hPa (Fig. 5), shows a predominately diurnal behavior in the Coriolis and advection terms, but not in the PGF term. The PGF is directed normal to the developing jet (not shown). As the elevated heating associated with the Ethiopian Highlands begins, air accelerates southeastward toward the mountains and gradually turns southwestward due to the Coriolis force. Horizontal advection is also important in this case. North of the averaging box, the wind remains northeasterly, and the northeasterlies progress southward into the box during the evening.

Overall, the nocturnal flow with the low-level jet is more nearly in geostrophic balance than the flow during the day. One can therefore think of the development of the jet as a geostrophic adjustment process. Alternatively, one can view the jet as resulting from the formation of a cyclonic lee vortex on the west side of the Ethiopian Highlands (Fig. 3b, Fig. 4b). The general character of partially blocked flow is clear from the splitting of easterlies around the Highlands (Figs. 3b, 4a,b). The lee vortex is evident in the lee of the northern flank of the Highlands. A similar nocturnal vortex mechanism was discussed by Davis *et al.* (2000) in the context of lee vortices in the Bight region of California. The single cyclonic vortex is characteristic of the response to large mountains where the Rossby number (U/fL) is less than or of order unity. At moderate Ro (and low-Froude number), the effects of rotation are important even though the region is relatively near the equator. adjust geostrophically as mentioned above.

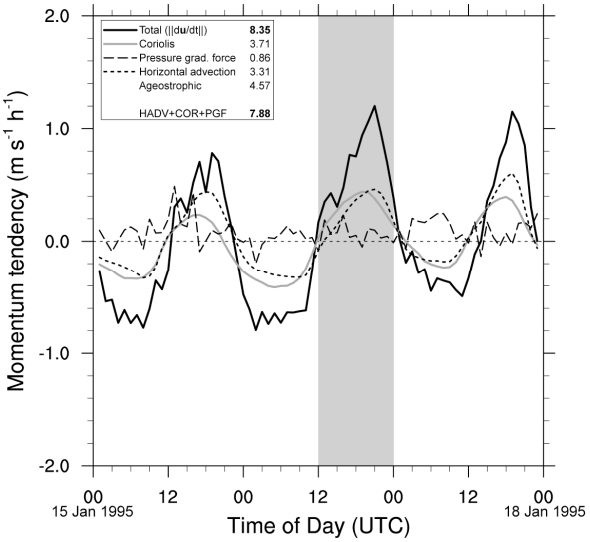

Figure 5. Time series of the individual terms in the horizontal momentum budget at 850 hPa, for the Ethiopia NLLJ for 15-18 Jan 1995, averaged over the acceleration region denoted by the gray lines in Fig. 4b. The vertical gray bar bounds the times of the plan view plots in Fig. 4a,b, and marks the interval over which the integrated acceleration is calculated for the various momentum terms, whose values are reported in the upper-left hand corner of the plot. The ageostrophic term is expressed as sum of the accelerations due to the pressure gradient force and the Coriolis force.

SUMMARY

This study has documented the characteristics of diurnally varying LLJs, ubiquitous features within the world's land covered areas that strongly drive the regional climate. A 21-year global downscaled reanalysis was created using NCAR's CFDDA, an MM5- and WRF-Model-based climate downscaling system. The uniqueness of this dataset is its hourly three-dimensional output, which allows us to fully resolve the diurnal cycle for any point on the globe. Moreover, CFDDA's 40 km grid spacing better resolves many of the physiographic features that drive the regional weather and climate compared to other widely available global reanalyses. The first quantitative global maps of NLLJs were created for this study, using a new index of NLLJ activity that is based on the vertical structure of the wind's temporal variation. Composite global maps of NLLJ activity were created that highlight not only the locations for recurring jets, but also their mean strength and direction, horizontal extent, geographic orientation, and amplitude of diurnal variation.

To conclude, although a basic mechanism of NLLJ formation has been understood for more than 40 years, the actual phenomenology of low-level jets is remarkably varied and much of this variety has escaped scrutiny until now. Horizontal heating contrasts, synoptic-scale transients and diurnal changes in boundary-layer turbulence combine to produce this rich variety of flow features. Most regions of the tropics or warm-season extratropics experience NLLJs on a regular basis. Furthermore, these jets have mesoscale and synoptic-scale extent. This implies that coherent transport can occur on scales of hundreds of kilometers overnight. The shallowness of the jets, their dependence on turbulence, their ubiquity and intensity underscore a fundamental challenge to global weather and climate modeling of the distribution of atmospheric constituents originating from the Earth's surface and human activity.

REFERENCES

Darby, L.S., K. J. Allwine, and R. M. Banta, 2006: Nocturnal low-level jet in a mountain basin complex. Part II: Transport and diffusion of tracer under stable conditions. *J. Appl. Meteorol. Climatol.*, **45**, 740-753.

Davis, C., S. Low-Nam, and C. Mass, 2000: *Dynamics of a Catalina Eddy Revealed by Numerical Simulation. Mon. Wea. Rev.*, **128**, 2885–2904.

Doyle, J. D., and T. T. Warner, 1993: A three-dimensional investigation of a Carolina low-level jet during GALE IOP 2. *Mon. Wea. Rev.*, **121**, 1030–1047.

Hahmann, A.N., D. Rostkier-Edelstein, T.T. Warner, Y. Liu, F. Vandenberg, Y. Liu, R. Babarsky, and S. P. Swerdlin, 2010: A reanalysis system for the generation of mesoscale climatographies. *J. Appl. Meteorol. Climatol*, in press.

Liu, Y., and Co-authors: The operational mesogamma-scale analysis and forecast system of the U.S. Army Test and Evaluation Command. Part 1: Overview of the modeling system, the forecast products, and how the products are used, *J. Appl. Meteor. Climatol.*, **47**, 1077–1092.

Mao, H., and R. Talbot, 2004: Role of meteorological processes in two New England ozone episodes during summer 2001. *J. Geophys Res. (D Atmos.).* **109**, doi:10.1029/2004JD004913.

Monaghan, A. J., D. L. Rife, J. O. Pinto, C. A. Davis, and J. R. Hannan, 2010: Global precipitation extremes associated with diurnally-varying LLJs. *J. Climate.*, provisionally accepted.

Rife, D.L., J.O. Pinto, A.J. Monaghan, and C.A. Davis, 2010: Global distribution and characteristics of diurnally-varying LLJs. *J. Climate*, provisionally accepted.

Salio, P., M. Nicolini, and E. J. Zipser, 2007: Mesoscale convective systems over southeastern South America and their relationship with the South American low-level jet. *Mon. Wea. Rev.*, **135**, 1290–1309.

Stensrud, D. J., 1996: Importance of low-level jets to climate. *J. Climate*, **9**, 1968-1711.

Stauffer, D. R. and N. L. Seaman, 1994: Multiscale 4-dimensional data assimilation. *J. Appl. Meteor.*, **33**, 416-434.

Stauffer, D. R., N. L. Seaman, and F. S. Binkowski, 1991: Use of 4-dimensional data assimilation in a limited-area mesoscale model. Part 2. Effects of data assimilation within the planetary boundary-layer. *Mon. Wea. Rev.*, **119**, 734-754.

Vera, C., J. Baez, M. Douglas, C. B. Emmanuel, J. Marengo, J. Meitin, Nicolini, J. Nogues-Paegle, J. Paegle, O. Penalba, P. Salio, C. Saulo, M. A. Silva Dias, P. Silva Dias, and E. Zipser, 2006: The South American Low-Level Jet Experiment. *Bull Amer. Meteor. Soc.*, **87**, 63–77